

Effect of quartz particle size on the mechanical behaviour of porcelain tile subjected to different cooling rates^{☆,☆☆}

Agenor De Noni Junior^{a,*}, Dachamir Hotza^b,
Vicente Cantavella Soler^c, Enrique Sanchez Vilches^c

^a Instituto Maximiliano Gaidzinski (IMG), 88845-000 Cocal do Sul, SC, Brazil

^b Universidade Federal de Santa Catarina (UFSC), 88040-900 Florianópolis, SC, Brazil

^c Instituto de Tecnología Cerámica (ITC), 12006 Castellón, Spain

Received 4 June 2008; received in revised form 30 July 2008; accepted 31 July 2008

Available online 27 September 2008

Abstract

Porcelain tile is a high-performance ceramic tile, in which quartz is a major compositional component. After the firing cycle, macroscopic residual stresses develop in the product as a result of rapid cooling. Further, during cooling, the presence of quartz particles also increases natural flaw size. Both phenomena significantly affect the product's mechanical behaviour. This study examines the effect of quartz particle size on the mechanical behaviour of porcelain tile subjected to two very different cooling rates: a rapid or a slow cooling rate. A series of porcelain tile compositions were designed for this purpose, in which quartz particle size was varied. The mechanical behaviour of the sintered pieces was evaluated on the basis of linear elastic fracture mechanics. It was verified that, in the slowly cooled material, the modulus of elasticity and fracture energy increased, and natural flaw size decreased as quartz particle size decreased. However, fracture energy also diminished in pieces that contained excessively small particles, with an advanced state of dissolution. For the rapidly cooled material, though the larger sized quartz particles debonded at higher temperatures owing to thermal stress, their presence, even in small quantities, contributed to natural flaw growth. The lower fracture energy associated with this last type of piece also favours this phenomenon.

© 2008 Elsevier Ltd. All rights reserved.

Keywords: Firing; Microstructure-Final; Mechanical Properties; Traditional Ceramics; Residual Stress

1. Introduction

Porcelain tile is a high-performance ceramic tile, whose composition resembles that of porcelain.^{1–3} However, the manufacturing process differs notably, particularly in regard to the firing stage, since porcelain tile firing cycles are much faster (40–60 min) than porcelain firing cycles (12–24 h).⁴ This rapid firing cycle conditions many porcelain tile end properties.

Previous research by the authors^{5,6} showed that porcelain tile is liable to develop macroscopic residual stresses when it is rapidly cooled, just as occurs in glass tempering.^{7,8} Since compressive surface stress was involved, mechanical strength was observed to increase. However, natural flaw size was also seen to augment significantly as the cooling rate increased, mainly because of the presence of crystalline quartz particles.⁶

Many studies on triaxial porcelains^{9–13} report that quartz significantly affects triaxial porcelain properties. On the one hand, the difference between the coefficients of thermal expansion of the quartz and of the glassy matrix has a strengthening effect by subjecting the glassy matrix to microscopic residual compressive stress. On the other hand, the magnitude of these stresses produces cracks around the quartz particles, which may exceed a critical size, thereby causing partial stress relaxation and increasing microstructural damage^{4,10,13}, which may even lead to particle detachment. This microstructural damage adversely affects the product's mechanical behaviour.

[☆] Based in part on the thesis submitted by A. De Noni Jr. for the Ph.D. degree in Materials Science and Engineering (PGMAT), Universidade Federal de Santa Catarina (UFSC), Brazil, 2007.

^{☆☆} This work was financially supported by the Brazilian Research Agency CAPES, under scholarship 2933-05-5 and co-financed by the Spanish Ministry of Industry, Tourism, and Trade for the Technology Institute Support Programme, under grant FIT-030000-2005-315/FIT-030000-2006-119.

* Corresponding author. Tel.: +55 48 3447 7736; fax: +55 48 3447 7736.

E-mail addresses: agenor@imgnet.org.br, agenordenoni@hotmail.com (A. De Noni Junior).

In porcelain tile, quartz particles play an even more important role since they constitute the most abundant crystalline phase in the end product. A previous study by the authors¹⁴ showed that the microscopic residual stresses exhibited by quartz particles were strongly affected by two factors: (1) the advanced state of dissolution of the smallest quartz particles, which modified the nature of the particle–matrix interface by increasing the state of stress on the particles; (2) the presence of a significant fraction larger than the critical particle size reduced the state of stress. It was further verified that the quartz in the porcelain tile matrix displayed an average coefficient of linear thermal expansion similar to that of the *c*-lattice parameter. This behaviour indicates that the process of quartz particle detachment from the matrix is encouraged by the anisotropic behaviour of quartz under thermal expansion.

This study seeks to determine the influence of quartz particle size on the mechanical behaviour of porcelain tile, evaluated on the basis of linear elastic fracture mechanics. The study has been conducted on a standard porcelain tile composition, in which the quartz particle size distribution was varied. In order to evaluate the influence of the cooling rate on mechanical behaviour, the samples were subjected to two different cooling cycles, either a faster or a slower cooling rate than those used in industrial practice.

2. Basic theoretical concepts

2.1. Mechanical strength of a material with a macroscopic residual stress profile

Application of the laws of linear elastic fracture mechanics allows mathematical description of the mechanical strength of a ceramic piece or plate with a macroscopic residual stress profile, σ_{ta} , subjected to bending stress, in accordance with Eq. (1).⁶

$$\sigma_{ta} = \frac{K_{IC}}{Ya^{1/2}} - \sigma_s \left(\frac{2S}{\pi} a + 1 \right) \quad (1)$$

where K_{IC} is the fracture toughness of the material without any macroscopic residual stress; σ_s , the macroscopic residual surface stress; $S = -6/h$, h the thickness of the piece; a , the size of the natural flaw; Y , a calibration factor, which in this case is 1.98.^{6,15}

For a material without any macroscopic residual stress, $\sigma_s = 0$, resulting from a slow cooling process, Eq. (1) is reduced to the Griffith equation, Eq. (2), to describe the bending strength (σ_f). All the parameters in Eq. (1), except natural flaw size (a), can be experimentally determined. The value of a can then be calculated using iterative methods. Fracture toughness is mathematically defined from Eq. (3).

$$\sigma_f = \frac{K_{IC}}{Y \cdot a^{1/2}} \quad (2)$$

$$K_{IC} = \sqrt{2E\gamma_i} \quad (3)$$

where E is the modulus of elasticity, and γ_i is the fracture energy of the material.

The factors that determine porcelain tile mechanical properties depend on tile composition and processing characteristics. However, microstructural damage and the state of microscopic stress caused by the quartz particles also decisively affect the modulus of elasticity¹⁶ and the fracture energy, respectively.¹⁷

Fracture energy is directly related to the greater or lesser ease with which fracture is able to propagate through the material. When the compressive stress on the glassy matrix and/or fracture surface tortuosity increases in porcelain tile, fracture energy may also be expected to increase.¹⁸

2.2. Critical particle size

Depending on the magnitude of the microscopic residual stresses, detachment of the particles from the matrix may occur at interface level, thereby increasing microstructural damage. Ito¹⁹ proposed a model, based on fracture mechanics, which could predict a critical particle diameter (d_c) above which such detachment would occur:

$$d_c = \frac{1}{0.15 \sin(\omega(2 - \sin \omega))} \frac{\gamma_{i,m}}{(\Delta\alpha \Delta T)\sigma_{rr}} \quad (4)$$

where $\gamma_{i,m}$ is the matrix fracture energy; ω , the relation of semi-spherical crack size to particle diameter, $\omega \sim 0.3$ would correspond to a typical value calculated by Ito;⁴ σ_{rr} is the radial stress on the particles; $\Delta\alpha$, the difference between the coefficients of linear thermal expansion of the particle and of the matrix; ΔT , the cooling temperature range, in the case of a glassy matrix this being from approximately glass transformation temperature (T_g) to ambient temperature (T_{amb}).

Applying Eq. (4) to estimate the critical sizes associated with each lattice parameter in the quartz unit cell yields a value of $\sim 6 \mu\text{m}$ for ‘*a*’ and a value of $\sim 44 \mu\text{m}$ for ‘*c*’, owing to the anisotropy of the coefficient of thermal expansion.²⁰ These results indicate that selective detachments may occur so that only particles larger than $\sim 44 \mu\text{m}$ would completely debond from the matrix, with fully relaxed stresses. In contrast, particles sized between ~ 6 and $\sim 44 \mu\text{m}$ (most particles in porcelain tile compositions) would be partly detached from the matrix. Other authors^{4,13} have confirmed the existence of partial peripheral cracks around particles larger than $5 \mu\text{m}$, and complete cracking around particles larger than $50 \mu\text{m}$.

This loss of contact occurs as the tile cools. The graph in Fig. 1 shows the critical diameter of quartz particles throughout the cooling, estimated from Eq. (4), based on the coefficients of thermal expansion of the *a*- and *c*-lattice parameters²⁰ (for the sake of simplification, the glass matrix fracture energy is assumed not to change with temperature, $\gamma_{i,m} = 3.5 \text{ J/m}^2$).

As the material cools, microscopic stress grows and the critical diameter consequently decreases until it reaches a minimum value at ambient temperature. However, the critical diameter for parameter ‘*a*’ drops significantly between 575 and 500 °C from $\sim 460 \mu\text{m}$ to $\sim 30 \mu\text{m}$, reaching $\sim 6 \mu\text{m}$ at 25 °C. The larger the quartz particle size in the porcelain tile, the sooner will particle detachment (and hence microstructural damage) occurs. In a previous study,⁶ the authors verified that

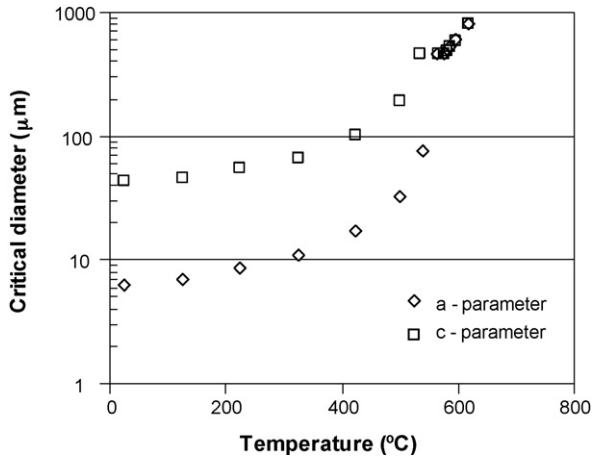


Fig. 1. Critical diameter, Eq. (4), of quartz particles as a function of cooling temperature, calculated for lattice parameters *a* and *c*.

such detachments in the presence of thermal tensile stresses at the surface encouraged natural flaw growth in the tested pieces.

3. Experimental procedure

Tests were performed using a porcelain tile composition made up of approximately 50% albite, 30% kaolinite, and 20% quartz, in which only quartz particle size was varied. A floated sodium feldspar (Kaltun) and Super Standard Porcelain kaolin (Imerys) were used as sources of albite and kaolinite, respectively. Four types of quartz with different particle size distributions, but with the same chemical and mineralogical composition, were used: SE500, SE100, SE12, and SE8 (Sibelco). The chemical compositions of the materials used are given in Table 1. The quartz samples with different particle sizes and the other components were then used to prepare mixtures PQ1, PQ2, PQ3, and PQ4 (ordered from smallest to largest quartz particle size), according to the standard porcelain tile formulation.

The quartz particle size distribution in the mixtures is shown in Fig. 2. The figure also indicates a table with dates for the median particle size (D50) and particle size for percentile 99th (D99) of each distribution. Approximately 17% of the quartz in the composition comes from the feldspar; the distributions therefore display differences with regard to commercial quartz. The feldspar quartz has a particle size distribution similar to that of SE100 quartz. As a result, in the mixture containing SE500 quartz (the finest particle size), the distribution exhibits

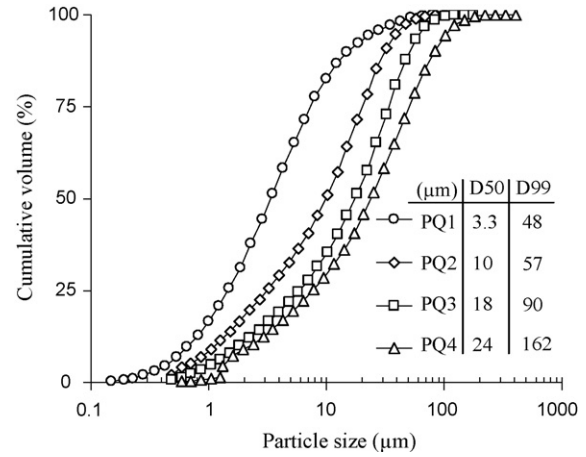


Fig. 2. Quartz particle size distribution in the mixtures.

maximum particle sizes similar to those of the mixture with SE100 quartz (Fig. 2).

The test mixtures (PQ1, PQ2, PQ3, and PQ4) were proportioned, homogenised by wet milling for 45 min, and then spray dried. Composition PQ2 was closest to the industrial mixtures, so that the remaining compositions amply covered the standard industrial range. The 80 mm × 20 mm × 7 mm samples were pressed at 45 MPa and 5.5% moisture content (dry weight basis). They were then dried in an oven at 110 °C and fired in an electric kiln at a heating rate of 70 °C/min from 25 to 500 °C, and 25 °C/min from 500 to 1230 °C, with a 6-min hold at peak temperature. The peak temperature used (1230 °C) corresponded to that of the maximum densification of the sintered piece (apparent density determined by the Archimedes principle). Only mixture PQ1 (finest quartz) was fired at 1220 °C, in order to maintain the maximum densification condition. Two types of cooling were used: one corresponding to cooling in the kiln, which was slower than that used in industry (~0.1 °C/s), and a second, faster type of cooling than that used in industry (~9.5 °C/s). In the second case, the samples were withdrawn from the furnace and subjected to an air stream to accelerate the cooling to approximately 650 °C, after which the fan was turned off and the pieces were isolated to reduce the cooling rate during the allotropic transformation of quartz (~3.6 °C/s). This procedure has been detailed elsewhere.⁶ Powders with particle size under 45 μm was prepared from fired samples in order to determine ultimate density, by helium pycnometry, to characterize the relative density (ρ , defined as ratio between apparent density of fire test piece and ultimate density of the powder).

Mechanical strength was determined, at room temperature, by three-point bend tests with a universal testing machine (Instron 6027) to which an extensometer (Instron Strain Gauge Extensometer 5 mm Range) was fitted in order simultaneously to determine the modulus of elasticity. Macroscopic residual stress was measured on a test piece from each type of cooling, using the strain relaxation method by incremental cuts,²¹ with a 4-mm-thick diamond-coated copper cutting disc and rectangular strain gauges (HBM with a 3-mm grid length). The fracture toughness of the material without residual stress (slow cooling) was determined by the SENB method (single-edge-notched

Table 1
Chemical composition of the materials used (% by weight)

	Feldspar	Kaolin	Quartz
SiO ₂	68	47	98.9
Al ₂ O ₃	19.2	38	0.51
Na ₂ O	10.9	0.15	0.01
K ₂ O	0.23	0.80	0.06
CaO	1.1	0.10	0.03
Others	0.34	0.64	0.11
LOI	0.14	13.0	0.27

Table 2
Mechanical characterisation of the test pieces subjected to slow cooling

Mixture	σ_f (MPa)	ρ	K_{IC} (MPa m ^{1/2})	E (GPa)	a_o (μm)	γ_i (J/m ²)	σ_q^* (MPa)	Wm
PQ1	69.8	0.977	1.49	55.2	115	19.6	346	23
PQ2	70.4	0.959	1.62	54.5	135	24.2	246	20
PQ3	63.5	0.955	1.57	49.3	155	25.0	214	37
PQ4	54.5	0.955	1.39	45.1	165	21.4	98	26

* Taken from Reference¹⁴.

beam). Fracture surface topography of the slowly cooled samples was characterised with a roughness meter (Hommelwerke model T8000). Polished surface porosity of the slowly cooled samples was determined with an optical microscope (Olympus bx 60) at 20 \times magnification; ten 550 μm \times 550 μm photographs were taken (JVC TK 1270E camera) and the images were analysed (Visilog 5.1 software). Finally, microstructural observation of the polished cross-sectional surfaces of some of the samples was carried out in a SEM.

4. Results and discussion

4.1. Porcelain tile subjected to slow cooling

Table 2 presents the results of the mechanical characterisation of the porcelain tile samples subjected to slow cooling: bending strength (σ_f); relative density (ρ); modulus of elasticity (E); fracture toughness (K_{IC}); natural flaw size (a) (calculated from Eq. (1)); fracture energy (γ_i) (calculated from K_{IC} and E); microscopic residual stress on the quartz particles¹⁴ (σ_q); and Weibull modulus (Wm).

The literature^{10–13} reports that the mechanical strength of porcelains increases as quartz particle size decreases. This was also the case in the tested porcelain tile mixtures, in which mechanical strength increased notably from mixture PQ4 (largest quartz particle size) to mixture PQ1 (smallest quartz particle size), though mixture PQ1 did not entirely follow the observed trend. The studies mentioned indicate that there is a minimum particle size that increases mechanical strength; however, they also report that below this particle size the foregoing trend even reverses.

For quantitative analysis of the role of each factor in the increase in mechanical strength, Griffith's equation (2), can be written as a Taylor series expansion truncate at first order term, making explicit a , E , and γ_i in three terms: δa , δE , and $\delta \gamma_i$, respectively, according to Eq. (5). The results are shown in Fig. 3.

$$\Delta\sigma_{fj} = \Delta E_j \left. \frac{\partial\sigma_f}{\partial E} \right|_{\bar{E}_j, \bar{\gamma}_{ij}, \bar{a}_j} + \Delta\gamma_{ij} \left. \frac{\partial\sigma_f}{\partial\gamma_i} \right|_{\bar{E}_j, \bar{\gamma}_{ij}, \bar{a}_j} + \Delta a_j \left. \frac{\partial\sigma_f}{\partial a} \right|_{\bar{E}_j, \bar{\gamma}_{ij}, \bar{a}_j} \quad (5)$$

$$\Delta\sigma_{fj}, \Delta E_j, \Delta\gamma_{ij}, \Delta a_j = \Delta X_j = X_j - X_{PQ4} \quad (6)$$

$$\bar{E}_j, \bar{\gamma}_{ij}, \bar{a}_j = \bar{X}_j = \frac{X_j + X_{PQ4}}{2} \quad (7)$$

$$\delta X_j = \Delta X_j \frac{\partial\sigma_f}{\partial X} \quad (8)$$

where j is any mixture (PQ1, PQ2, PQ3); data were taken from Table 2.

The results of Fig. 3 show that the three factors have practically the same degree of importance, so that variations in any of these factors would significantly change the increase in mechanical strength.

With regard to natural flaw size, Bragança et al.¹⁰ found that, for porcelain, this property was related to the size of the largest quartz particles in the distribution, which was also noted in mixture PQ4 (Fig. 2). For distributions with smaller particle sizes, the estimated flaw size is larger than the size of the largest particles in the distribution. In this case, Bragança et al. attributed natural flaw size to the interconnection of microcracks between neighbouring particles. The presence of large particles at the surface and the interconnection of microcracks both depend on probabilistic factors. It is reasonable, therefore, that natural flaw size should tend to decrease as quartz particle size is reduced, as the results show.

On the other hand, an increase in the modulus of elasticity stems from a rise in relative density²² and a drop in microstructural damage to the material,¹⁶ since the number of particles below the critical diameter also decreases when quartz particle size becomes smaller.

The lower tendency to increase mechanical strength in mixture PQ1 is clearly related to the observed decrease in fracture energy. As indicated elsewhere,¹⁴ about 20% of the initial quartz dissolves in mixture PQ1. This solution produces a layer rich in

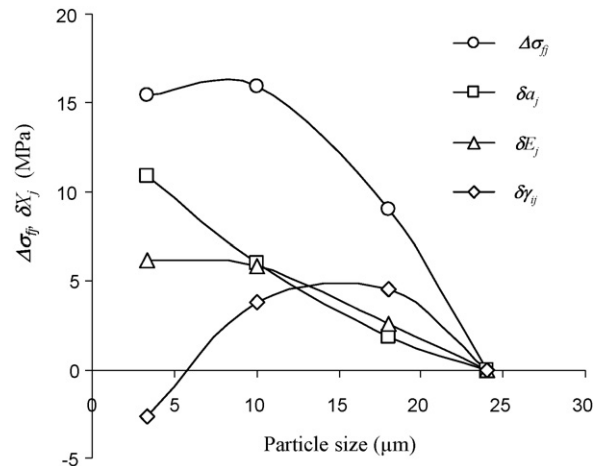


Fig. 3. Contribution of a , E , and γ_i on the increase in mechanical strength, $\Delta\sigma_{fj}$, as a function of median particle size of quartz.

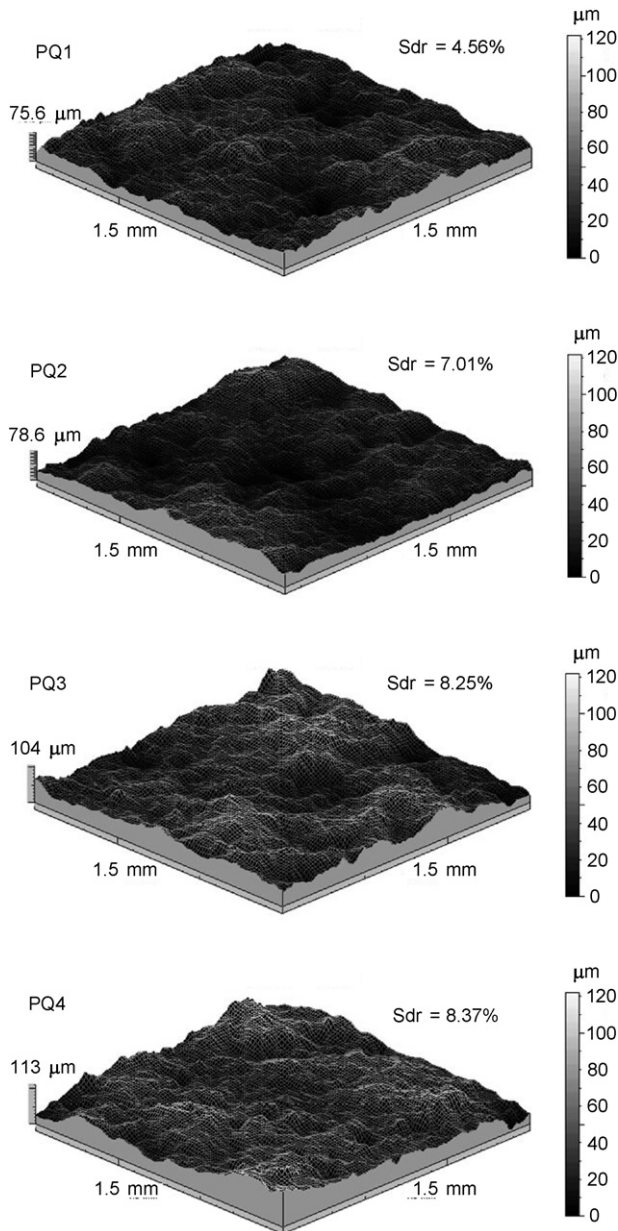


Fig. 4. Topography of the fracture surfaces in the slowly cooled samples.

amorphous silica around the quartz particles, a layer that raises the tensile stress on both the quartz particles and the glassy matrix, which reduces the strengthening effect of the remaining quartz particles. The general state of residual stress on the glassy matrix significantly affects the fracture energy of the material, since fracture mainly propagates through the matrix. Apart from mixture PQ1, the strengthening produced by the quartz particles may be indirectly observed through the microscopic residual stresses measured for these particles. The decreased fracture energy in porcelains obtained from quartz with a fine particle size has also been reported by other authors.¹⁰

Another factor that affects fracture energy is related to fracture propagation tortuosity. Fig. 4 shows the result of the topographic characterisation test of the fracture surface. It also includes the values obtained for parameter Sdr, which represents

Table 3

Mechanical characterisation of the test pieces subjected to rapid cooling

Mixture	σ_{ta} (MPa)	σ_s (MPa)	a (μm)	Wm	Δa (μm)
PQ1	89.8	31	150	22	35
PQ2	87.5	24	154	27	19
PQ3	77.5	22	185	23	30
PQ4	63.9	17	213	18	48

the increase in actual surface area in relation to the projected area ($1.5 \text{ mm} \times 1.5 \text{ mm}$)²³ (Sdr = 0% represents a perfect linear fracture, with no crack deflection). Sdr is observed to increase as quartz particle size increases; therefore, so does tortuosity.

Finally, when the fracture energy values are compared with the state of stress of the glassy matrix and with parameter Sdr, the importance of these two factors for this property can be clearly observed. Comparison of PQ3 with PQ2 indicates that the smaller strengthening effect on the matrix by the quartz particles is offset by the increased tortuosity. However, for mixture PQ4, the increase in tortuosity was insufficient to offset the smaller strengthening effect of the quartz particles, many more of which have debonded from the matrix ($\sim 80\% > 6 \mu\text{m}$ and $\sim 30\% > 44 \mu\text{m}$). Mixture PQ1 displays smaller tortuosity, as well as less strengthening stress by the quartz particles, owing to pronounced particle dissolution.

4.2. Porcelain tile subjected to rapid cooling

The mechanical characterisation data of the rapidly cooled porcelain tile pieces are presented in Table 3: mechanical strength (σ_{ta}); macroscopic residual surface stress (σ_s); natural flaw size (a); Weibull modulus (Wm); and the increase in natural flaw size related to slow cooling (Δa).

The mechanical strength values for the rapidly cooled pieces increased between 7 and 11 MPa compared with those subjected to slow cooling. This behaviour is due to the development of compressive macroscopic residual stress at the surface of the pieces, as indicated in section 1. However, this increase was lower than was to be expected on the basis of the measured residual stresses, owing to a simultaneous increase in natural flaw size.

As indicated above, the presence of disperse quartz particles in the matrix decisively affects the generation of the natural flaw in slowly cooled pieces. After the allotropic transformation of quartz (573°C), the particles undergo pronounced shrinkage, which increases microscopic stresses. Fig. 1 shows that, as the piece cools, the particles begin to debond from the matrix, giving rise to peripheral cracks. When the cooling is rapid, thermal tensile stresses form at the surface; peripheral cracks thus encounter more favourable growth conditions, which lead to an increase in natural flaw size. The larger the particles, the sooner will they debond from the matrix (i.e. at higher temperatures) and, therefore, the greater will their growth be.

This mechanism accounts for the higher values of Δa as quartz particle size increases in mixtures PQ2, PQ3, and PQ4. The same occurs with mixture PQ1. However, in this case two features may be noted: (1) though the average quartz particle

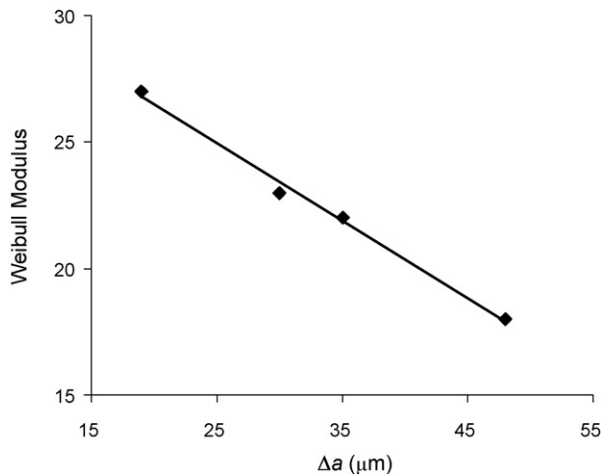


Fig. 5. Relation between the Weibull modulus and the increase in natural flaw size of the rapidly cooled test pieces with regard to slowly cooled pieces.

size is smaller than in the other mixtures, the largest sizes (D99, Fig. 2) are practically the same as in mixture PQ2 as a result of the quartz from the feldspar, so that the first detachments occur at the same temperature as in PQ2; (2) the fracture energy is smaller than in the other mixtures, which constitutes a more favourable condition for crack growth. The negative effect caused by a small number of large-sized particles has also been noted by other authors.¹¹

The samples subjected to slow cooling displayed no clear tendency in the Weibull modulus in relation to quartz particle size or natural flaw size. A linear relationship was observed, however, between the Weibull modulus and the increase in natural flaw size for rapidly cooled pieces with regard to slowly cooled pieces (Fig. 5). This trend indicates that the greater the microstructural damage that occurs in rapid cooling cycles, the lower will the Weibull modulus and the greater will the variability be in the flaw population in the pieces (the Weibull modulus is related to the amplitude of the flaw size distribution²⁴).

4.3. Comparison between microstructures formed in the pieces subjected to the two types of cooling

Microscopic observation of peripheral crack growth around the quartz particles is very complicated, since polishing during the sample preparation process is a further cause of microstructural damage. However, two materials with differing initial states of damage, subjected to the same polishing conditions, may also be expected to exhibit different ensuing microstructural damage. The micrographs shown in Fig. 6 correspond to samples of mixture PQ2 (the closest to industrial compositions), subjected to the two tested types of cooling. All system features can be quite clearly observed in both cases: closed porosity (P), quartz particles (Q), albite particles (A), albite glass (VA), primary mullite (M), and kaolin glass (VC). The quartz particles in both cases are approximately the same size. However, the rapidly cooled test piece displays a more damaged microstructure owing to thermal tensile stress at the surface during cooling. This differentiation is not widely

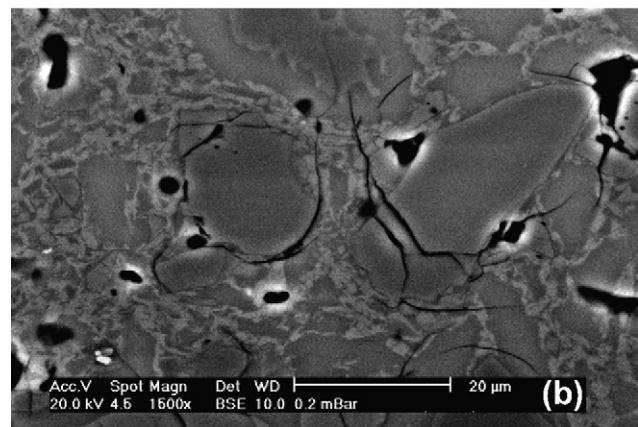
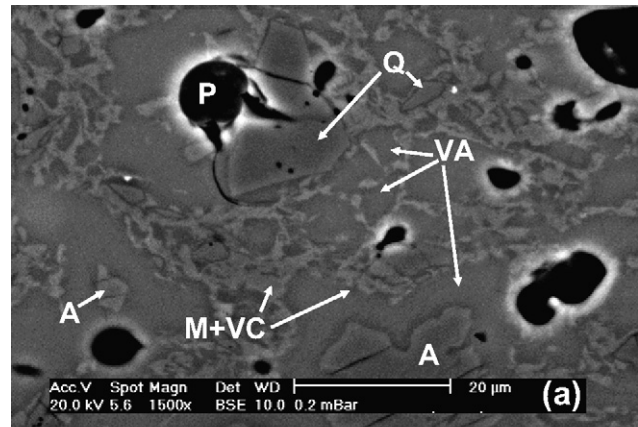


Fig. 6. Micrographs of samples made from mixture PQ2 subjected to (a) slow, and (b) rapid cooling.

observed, however, in all the areas near the surface of the piece.

4.4. Analysis of surface porosity in the polished pieces

Porosity in a polished porcelain tile surface directly affects porcelain tile aesthetic characteristics, such as gloss and cleanability.²⁵ Fig. 7 presents a graph that relates surface porosity (percentage of surface area occupied by pores) to the inner

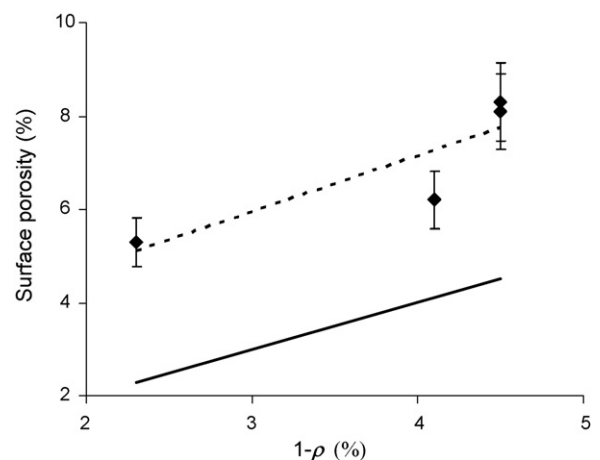


Fig. 7. Relation between surface porosity and inner porosity of the material.

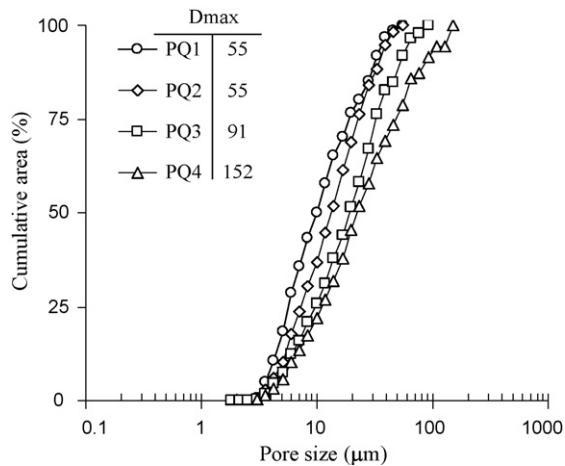


Fig. 8. Pore size distribution in the polished surface.

porosity of the material ($1 - \rho$). The solid line represents the situation in which surface porosity is equal to inner porosity. It may be observed that polished surface porosity is higher than the material's inner porosity. In addition to increasing microstructural surface damage, polishing also causes particle debonding, which increases surface open porosity.

The graph in Fig. 8 presents the size distribution of the surface pores for the samples and the maximum pore size (D_{\max}). The plots show that as the quartz particle size increases (Fig. 2), surface pore size also increases. For the samples, maximum pore size is directly related to the coarsest fraction of the particle size distribution, since the pore size values coincide with the particle sizes that cut the cumulative distribution at $\sim 99\%$ (Fig. 2) in every case. These results indicate that it is the quartz particles that detach themselves most easily owing to the presence of peripheral cracks around them and, therefore, that they largely determine the surface characteristics of polished porcelain tiles. These results indicate once again the importance of the coarse quartz particle fraction, as was observed in the growth of natural flaw size.

5. Conclusions

Porcelain tile properties have been determined on the basis of linear elastic fracture mechanics. Quartz particle size was varied in the pieces, and the tiles were subjected to either rapid or slow cooling.

A decrease in quartz particle size was observed to increase the modulus of elasticity and to decrease natural flaw size. Fracture energy increased as a result of microstructural strengthening by the quartz particles and the increased tortuosity of the fracture surface. However, excessively small particles, which display an advanced state of dissolution, give rise to interfaces rich in amorphous silica between the matrix and the particle, decreasing the strengthening effect of the remaining quartz.

The increase in natural flaw size observed in the rapidly cooled pieces was due to the thermal tensile stress at the tile surface and to the presence of quartz particles. In addition, the largest particles debonded at higher temperatures and encour-

aged natural flaw growth. Finally, it was verified that the lower the fracture energy of the material, the greater was the increase in natural flaw size during rapid cooling.

The increase in surface porosity of polished pieces with respect to the inner porosity of the material was closely related to quartz particle detachment. The coarse quartz particle size fraction therefore determined maximum surface pore size.

Acknowledgments

The authors wish to thank the staff at the Instituto de Tecnología Cerámica (ITC), Spain; the Coordination for the Improvement of Higher Education Personnel (CAPES), Brazil; and the Instituto Maximiliano Gaidzinski (IMG), Brazil. The authors also thank the Spanish Ministry of Industry, Tourism, and Trade for co-financing the Technology Institute Support Programme (FIT-030000-2005-315/FIT-030000-2006-119).

References

- Sánchez, E., Orts, M. J., Ten, J. G. and Cantavella, V., Porcelain tile composition: effect on phase formation and end products. *Am. Ceram. Soc. Bull.*, 2001, **80**, 43–49.
- Cavalcante, P. M. T., Dondi, M., Ercolani, G., Guarini, G., Melandri, C., Raimondo, M. *et al.*, The influence of microstructure on the performance of white porcelain stoneware. *Ceram. Int.*, 2004, **30**, 953–963.
- Manfredini, T., Pellacani, G. C. and Romagnoli, M., Porcelainized stoneware tile. *Am. Ceram. Soc. Bull.*, 1995, **74**, 76–79.
- Senapati, U. and Carty, W. M., Porcelain-raw materials, processing, phase evolution, and mechanical behavior. *J. Am. Ceram. Soc.*, 1998, **81**, 3–20.
- De Noni Jr., A., Hotza, D., Cantavella, V. and Sánchez, E., Influencia del enfriamiento de la etapa de cocción sobre las propiedades mecánicas del gres porcelánico. *Bol. Soc. Esp. Ceram. V.*, 2007, **46**(4), 163–170.
- De Noni Jr., A., Hotza, D., Cantavella, V. and Sánchez, E., Influence of macroscopic residual stresses on the mechanical behavior and microstructure of porcelain tile. *J. Eur. Ceram. Soc.*, 2008, **28**, 2463–2469.
- McMaster, R. A., Fundamentals of tempered glass. *Ceram. Eng. Sci. Proc.*, 1989, **10**, 193–206.
- Navarro, J. M. F., *El vidrio, constitución, fabricación y propiedades*. CSIC, Madrid, 2003.
- Stathis, G., Ekonomakou, A., Stournaras, C. J. and Ftikos, C., Effect of firing conditions, filler grain size and quartz content on bending strength and physical properties of sanitaryware porcelain. *J. Eur. Ceram. Soc.*, 2004, **24**, 2357–2366.
- Bragança, S. R., Bergmann, C. P. and Hübner, H., Effect of quartz particle size on the strength of triaxial porcelain. *J. Eur. Ceram. Soc.*, 2006, **26**, 3761–3768.
- Hamano, K., Wu, Y. H., Nakagawa, Z. and Hasegawa, M., Effect of coarse quartz grain on mechanical strength of porcelain body. *J. Ceram. Soc. Jap. Int. Ed.*, 1991, **99**, 1070–1073.
- Hamano, K., Wu, Y. H., Nakagawa, Z. and Hasegawa, M., Effect of grain size of quartz on mechanical strength of porcelain bodies. *J. Ceram. Soc. Jap. Int. Ed.*, 1991, **99**, 149–153.
- Warshaw, S. I. and Seider, R. J., Comparison of strength of triaxial porcelains containing alumina and silica. *J. Am. Ceram. Soc.*, 1967, **50**, 337–342.
- De Noni Jr., A., Hotza, D., Cantavella, V. and Sánchez, E., Analysis of the development of microscopic residual stresses on quartz particles in porcelain tile. *J. Eur. Ceram. Soc.*, 2008, **28**, 2629–2637.
- Slavo, V. M., Larentis, L. and Green, D. J., Flaw-insensitive ion-exchanged glass: I, theoretical aspects. *J. Am. Ceram. Soc.*, 2001, **84**, 1827–1831.
- Stubna, I., Trnák, A. and Vozár, L., Thermomechanical analysis of quartz porcelain in temperature cycles. *Ceram. Int.*, 2007, **33**, 1287–1291.

17. Marshall, D. B. and Evans, A. G., The influence of residual stress on the toughness of reinforced brittle materials. *Mater. Forum*, 1988, **11**, 304–312.
18. Evans, A. G., Perspective on the development of high-toughness ceramics. *J. Am. Ceram. Soc.*, 1990, **73**, 187–206.
19. Ito, Y. M., Rosenblatt, M., Cheng, L. Y., Lange, F. F. and Evans, A. G., Cracking in particulate composite due to thermalmechanical stress. *Int. J. Fract.*, 1981, **17**, 483–491.
20. Kihara, K., An X-ray study of the temperature dependence of the quartz structure. *Eur. J. Miner.*, 1990, **2**, 63–77.
21. Lu, J., *Handbook of Measurement of Residual Stress*. Fairmont Press, Lilburn, 1996.
22. Callister Jr., W. D., *Materials Science and Engineering: An Introduction (Sixth edition)*. John Wiley, New York, 2005.
23. Liam Blunt and Xiangqian Jian, ed., *Advanced Techniques for Assessment Surface Topography*. Kogan Page Science, London and Sterling, 2003.
24. Torrecillas, R. and Moya, J. S., Mecánica de fractura en materiales cerámicos frágiles: Principios fundamentales. *Bol. Soc. Esp. Ceram. Vidr.*, 1988, **27**(3), 123–134.
25. Sánchez, E., Ibáñez, M. J., García-Ten, J., Quereda, M. F., Hutchings, I. M. and Xu, Y. M., Porcelain tile microstructure: implications for polished tile properties. *J. Eur. Ceram. Soc.*, 2006, **26**(13), 2533–2540.